CellPress
Neuron
Report

Refinement of the Retinogeniculate Synapse by Bouton Clustering

Y. Kate Hong,[1,2,3] SuHong Park,[1] Elizabeth Y. Litvina,[1] Jose Morales,[1] Joshua R. Sanes,[2] and Chinfei Chen[1,*]
[1]F.M. Kirby Neurobiology Center, Department of Neurology, Boston Children's Hospital, Harvard Medical School, 300 Longwood Avenue, Boston, MA 02115, USA
[2]Department of Molecular and Cellular Biology, Center for Brain Science, Harvard University, 52 Oxford Street, Cambridge, MA 02138, USA
[3]Present address: Department of Neuroscience, Columbia University, New York, NY 10032, USA
*Correspondence: chinfei.chen@childrens.harvard.edu
http://dx.doi.org/10.1016/j.neuron.2014.08.059

SUMMARY

Mammalian sensory circuits become refined over development in an activity-dependent manner. Retinal ganglion cell (RGC) axons from each eye first map to their target in the geniculate and then segregate into eye-specific layers by the removal and addition of axon branches. Once segregation is complete, robust functional remodeling continues as the number of afferent inputs to each geniculate neuron decreases from many to a few. It is widely assumed that large-scale axon retraction underlies this later phase of circuit refinement. On the contrary, RGC axons remain stable during functional pruning. Instead, presynaptic boutons grow in size and cluster during this process. Moreover, they exhibit dynamic spatial reorganization in response to sensory experience. Surprisingly, axon complexity decreases only after the completion of the thalamic critical period. Therefore, dynamic bouton redistribution along a broad axon backbone represents an unappreciated form of plasticity underlying developmental wiring and rewiring in the CNS.

INTRODUCTION

In many developing mammalian neural circuits, connections are refined over development with synapse elimination and strengthening. The canonical view of refinement involves large-scale retraction of axons. This view is derived in large part from studies of peripheral motor and autonomic axons (Keller-Peck et al., 2001; Purves and Lichtman, 1980; Tapia et al., 2012). In only a few cases have axonal dynamics been analyzed during circuit refinement in the CNS (Cheng et al., 2010; Hashimoto et al., 2009; McLaughlin et al., 2003; Sugihara, 2005). It therefore remains unclear whether the model of axon retraction applies generally to central projections.

Here, we use the retinogeniculate synapse to address this issue. Initially, retinal ganglion cell (RGC) axons from each eye form imprecise maps in the dorsal lateral geniculate nucleus (LGN), with individual axons innervating neurons across eye-specific layers with a broad retinotopic expanse. By adulthood, these maps are retinotopically precise with axons targeted to specific monocular layers and low afferent convergence onto geniculate neurons. This transformation occurs in at least three phases (Figure 1A). First, axonal arbors become topographically refined and segregate into eye-specific layers (Dhande et al., 2011; Sretavan and Shatz, 1984). In mice, this phase occurs by approximately postnatal day 10 (~P10) (Hong and Chen, 2011; Huberman et al., 2008), prior to eye opening at ~P12. Second, continuing until ~P20, functional studies show that the number of axons that innervate each LGN neuron decreases several-fold (synapse elimination) and the connections that persist become stronger (synaptic strengthening) (Chen and Regehr, 2000; Jaubert-Miazza et al., 2005). This phase, like the first, depends on spontaneous activity but not vision. Third, refinement continues and becomes dependent on visual experience between P20 and P30. Visual deprivation during this phase (referred to as late dark rearing [LDR]) reduces synaptic strength and increases the number of afferent RGC inputs onto relay neurons (Hooks and Chen, 2006, 2008).

Classical studies have analyzed structural correlates of the first phase of refinement in several mammalian species. Axons segregate into eye-specific layers by the removal of sprouts from "incorrect" layers and elaboration of new branches and synapses in "correct" layers (Sretavan and Shatz, 1984). Little is known, however, about structural alterations that underlie later phases. Here, to elucidate the structural basis for changes in functional connectivity during development, we used transgenic mice in which a functionally defined subset of RGCs (BD-RGCs) can be sparsely labeled (Kim et al., 2010), and reconstructed individual RGC arbors over development and in response to sensory deprivation. We find that rather than axon retraction, changes in presynaptic bouton size and distribution underlie late synaptic refinement and experience-dependent plasticity at the retinogeniculate synapse. Structural pruning does occur, however, during a fourth, previously unrecognized phase of refinement that follows the period for vision-directed plasticity. Together, our results suggest that bouton rearrangement, rather than arbor pruning, underlies functional refinement and that axon retraction serves to limit synaptic plasticity in the adult.

RESULTS

To visualize RGC axon arbors, we used transgenic mice that express a tamoxifen-activated Cre recombinase (CreER) in BD-RGCs, which are bistratified, ON-OFF direction-selective

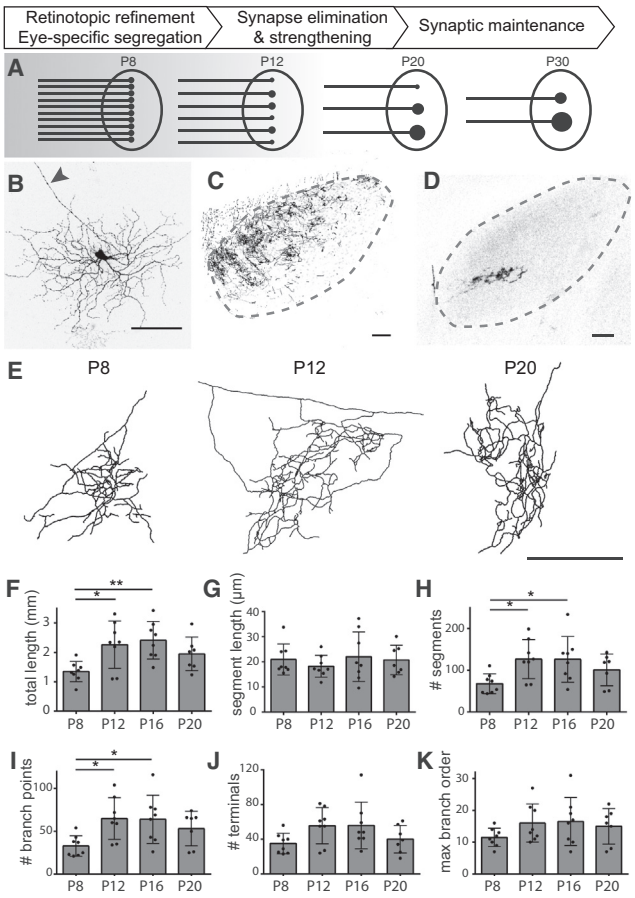

Figure 1. Development of BD-RGC Axon Terminals in the LGN

(A) Schematic of functional pruning at the retinogeniculate synapse. LGN neurons (large ovals) and RGC inputs (black lines) of varying strength (black circles). Adapted from Hong and Chen (2011). (B) Confocal images of BD-RGC labeled in the retina of BD-YFP double transgenic mice. Arrowhead: primary axon. (C) Dense labeling of BD-RGC axons in the dorsolateral region of LGN (sagittal view). (D) Single axon labeled by low dose of tamoxifen. Dashed lines indicate LGN boundary. (E) Examples of reconstructed BD-RGC axon arbors. (F–K) Quantification of (F) total axon length, (G) average segment length, number of (H) segments, (I) branch points, (J) terminal endings, and (K) maximum branch order. (B–D) Image gray values inverted for clarity. Scale bars represent 100 μm. Error bars indicate SEM. See also Figure S1.

cells that respond to downward motion (Kim et al., 2010). When these mice are crossed to mice in which expression of YFP is Cre dependent (Buffelli et al., 2003), BD-RGCs are indelibly marked following administration of tamoxifen. The use of ligand-activated Cre allowed us to control the number of cells labeled in the retina by titrating the dose of tamoxifen administered and thus visualize single-cell morphology (Figures 1B–1E). BD-RGC axon arbors target the area where we and others have previously characterized retinogeniculate synaptic refinement by slice electrophysiology (Chen and Regehr, 2000; Jaubert-Miazza et al., 2005; Koch and Ullian, 2010; Stevens et al., 2007). By focusing on one RGC subtype, structural heterogeneity arising from the existence of multiple RGC subtypes can be minimized. Our analysis was restricted to arbors that projected to the dorsal lateral portion of the LGN (Figures S1A and S1B available online), which spans both the shell and core regions of the LGN (Cruz-Martín et al., 2014; Krahe et al., 2011).

Spontaneous Activity-Dependent Phase of Structural Refinement

We first analyzed axons between P8 and P20, which spans the last days of eye-specific segregation (nearly complete by P10), eye opening (P12–P14), and experience-independent synapse elimination (Hong and Chen, 2011; Huberman, 2007). The number of afferent inputs per relay neuron decreases from >10 to half during this period, and the remaining inputs strengthen ~20-fold (Chen and Regehr, 2000; Hooks and Chen, 2006).

Surprisingly, average arbor size and complexity did not decrease during this period. Instead, the axon total length and complexity increased significantly between P8 and P12 (Figures 1F, 1H, and 1I), consistent with previous observations (Dhande et al., 2011; Snider et al., 1999; Sretavan and Shatz, 1984). While this period of axon expansion corresponds to growth of the LGN (Figure S1C), the estimated number of LGN neurons encompassed by a single BD-RGC axon arbor volume did not change significantly (Figures S1D–S1F). Arbor growth between P8 and P12 was also concurrent with an increase in the number of branch points (Figure 1I), suggesting elaboration of the arbor and increase in potential contacts between pre- and postsynaptic partners. Between P12 and P20, a period of active functional synapse elimination, there was little change in the total or average segment length, number of segments, branch points, terminals, or branch order of arbors (Figures 1F–1K). Together, these results reveal dissociation between functional synaptic elimination and structural pruning.

Spatial Redistribution of Presynaptic Boutons Occurs with Development

Detailed examination of the reconstructed arbors provided insight into the structural basis of developmental refinement. The most striking changes between P8 and P20 were in the size and location of bouton-like varicosities along the axon terminal (Figures 2A–2C). We defined boutons as regions of the arbor where the width of axons was greater than twice the diameter of the flanking axon (Supplemental Experimental Procedures). The average bouton diameter increased significantly between P8 and P20 ($p < 0.001$, Kruskal-Wallis one-way ANOVA and Dunn's post hoc test; Figure 2L; Figures S2A–S2C). Previous ultrastructual studies have indicated that in the adult LGN, the number of release sites is correlated to the volume of boutons (Hamos et al., 1987). Thus, an increase in bouton size may correspond to the addition of synapses within each bouton as connections are strengthened over development.

In order to determine whether structural boutons contained presynaptic elements, we quantified the degree of colocalization of boutons with vesicular glutamate transporter 2 (VGLUT2), a presynaptic marker for RGC, but not cortical, inputs in the LGN (Land et al., 2004) (Figures 2D–2I). Colocalization was high at both immature and mature axons and did not significantly differ with age (88.2% ± 4.1% at P8 versus 92.5% ± 6.5% at P20–P30, SD, $p = 0.09$, Student's t test, $n = 10$, statistical power = 0.8; Supplemental Experimental Procedures; Figure S2G). We also

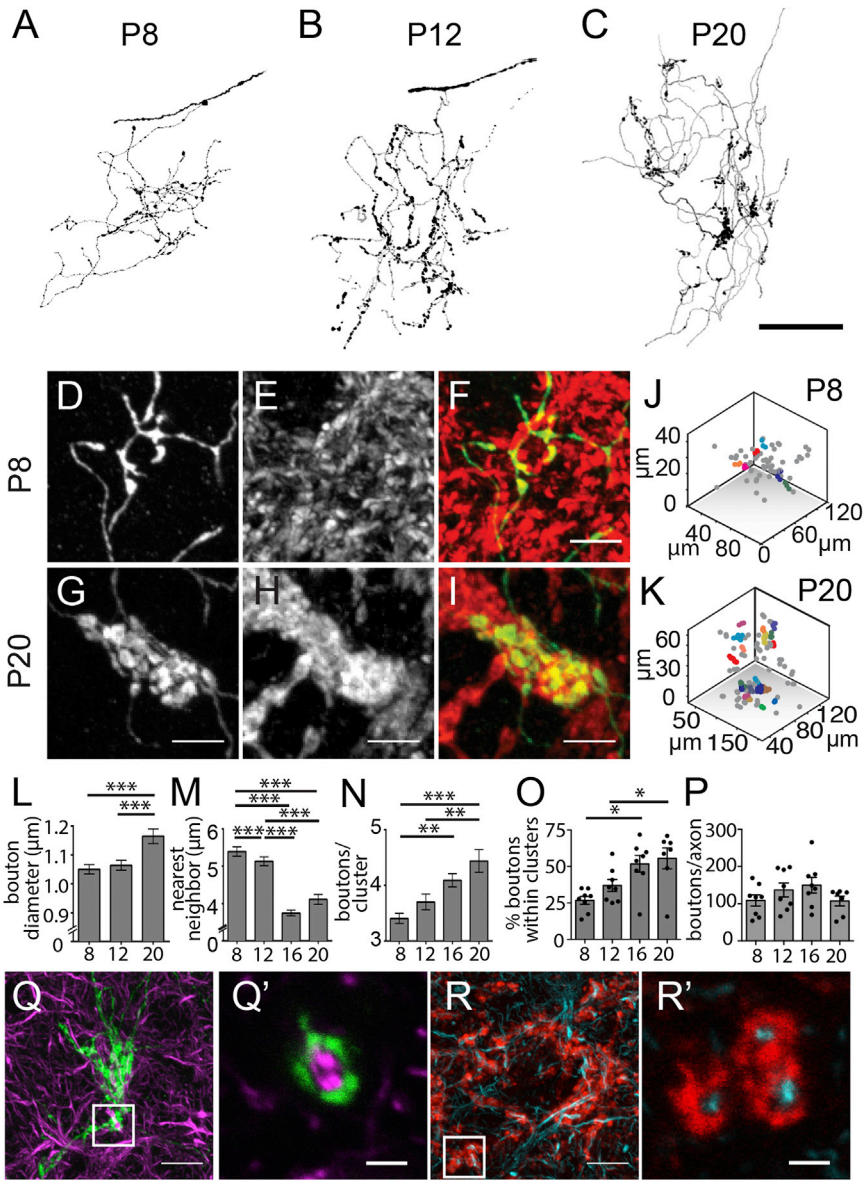

Figure 2. Boutons Cluster over Development

(A–C) Confocal images of single YFP-labeled BD-RGC axons at different ages. (D–I) LGN from P8 and P20 BD-YFP mice coimmunolabeled against YFP (D and G), VGLUT2 (E and H), and merged images (F and I; VGLUT2, red; YFP, green). (J and K) Example outcomes of mean-shift clustering analysis for boutons in x, y, z space for axons shown in (A) and (C). Colored dots represent boutons within clusters; gray dots lie outside clusters. (L–P) Quantification of bouton diameter (L), NN distances (M), cluster size (boutons/cluster, >2 boutons) determined by mean-shift clustering analysis (N), percentage of boutons within clusters (O), and number of boutons per axon (P). x axis: postnatal day. (Q–R′) Maximum projection images of confocal stacks of P22 LGN labeling BD-RGC (green) and SMI-32 (magenta) (Q and Q′); VGLUT2 (red) and SMI-32 (cyan) (R and R′). (Q′) and (R′) are magnified images of single optical section of inset shown in (Q) and (R), respectively. Scale bars represent 50 μm in (A)–(C), 5 μm in (D)–(I), 10 μm in (Q) and (R), and 2 μm in (Q′) and (R′). Error bars indicate SEM. See also Figures S2 and S3.

quantified the fraction of VGLUT2-positive puncta within BD axons that did not colocalize to boutons. This may reflect less mature synapses or trafficking of synaptic elements along the axon early in development. Consistent with this notion, the fraction of VGLUT2 puncta outside of boutons was significantly higher in young than old axons (18.5% ± 8.0% versus 10.9% ± 5.1%, SD, n = 10, p = 0.02; Figure S2G). Thus, over development, varicosities are reliable markers for presynaptic boutons representing more mature synapses.

In addition to size, the spatial distribution of boutons changed dramatically as the synapse matured. At P8, boutons were relatively evenly dispersed throughout the axon arbor. In contrast, by P20, boutons were densely clustered in restricted regions of the axon, leaving large stretches of the axon arbor without boutons (Figures 2A–2C; Figures S3G and S3H). We determined the 3D x, y, and z positions of each bouton along the arbor of singly labeled axons (Figures 2J and 2K) and quantified clustering in two ways: nearest neighbor distance and mean-shift clustering (see Supplemental Experimental Procedures). The average nearest neighbor (NN) distance decreased significantly from ~5.5 μm at P8 to ~4 μm at P20, by which point clusters of boutons are visibly discernible (Figures 2A–2C and 2M). Likewise, cluster size and the percent of boutons within clusters gradually increased between P8 and P20 (Figures 2N and 2O). Despite the spatial redistribution of boutons with maturation, the average number of boutons/arbor remained unchanged over development (Figure 2P). Taken together, our results suggest that an immature RGC makes weak synaptic contacts broadly onto many LGN neurons within the territory covered by its arbor, and functional retinogeniculate refinement occurs by spatially redistributing a limited number of boutons over a broad axon scaffold such that they are concentrated onto a few postsynaptic neurons.

Coimmunolabeling revealed that YFP-positive bouton clusters were frequently nested within a larger cluster of VGLUT2 islands (Figures 2G–2I; Figures S2D–S2F). This suggests that single axon arbor clusters were part of larger groups of boutons contributed by other, unlabeled RGC axons. As VGLUT2 is expressed in most RGC terminals (Land et al., 2004), of which a minority are BD-RGCs (~4% of RGCs in the retina; Kay et al., 2011), bouton clustering is probably a general mechanism used by other RGC types. The bouton clusters were frequently found to form rosette- or donut-like structures (Figures S2D–S2F, S2H,

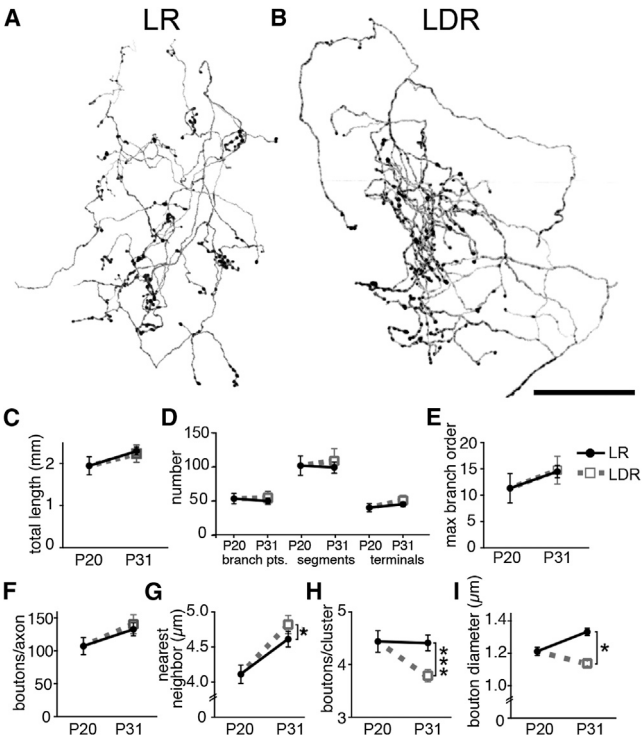

Figure 3. Sensory-Dependent Axonal Remodeling

Maximum projection images of (A) LR and (B) LDR BD-RGC axons. Quantification of average axon (C–E) and bouton (F–I) parameters between P20 and P31 in LR (black) and LDR (gray) mice. P20 data set is the same as in Figures 1 and 2, shown for comparison. Scale bars represent 50 μm. Error bars indicate SEM.

and S2I) in which the "holes" contained processes labeled by antibodies against unphosphorylated neurofilament (SMI-32), a marker of somata and proximal dendrites of LGN neurons, (Figures 2Q–2R′; Jaubert-Miazza et al., 2005). Thus, clustering is likely to reflect numerous synapses from one or a few cells onto proximal dendrites of relay neurons (Hamos et al., 1987). RGC inputs that contribute to the same cluster may be functionally similar, as suggested by studies in other regions of the CNS (Winnubst and Lohmann, 2012).

Experience-Dependent Anatomical Refinement

The vision-independent developmental period is followed by a later phase of experience-dependent plasticity spanning P20–P31. Under normal light-rearing (LR) conditions (12 hr light/dark cycle), visual experience stabilizes and maintains the refined circuitry, and electrophysiological studies show no substantial changes in strength or connectivity between P20 and P31. However, extreme changes in visual experience, such as dark rearing during this period (from P20 for >7 days, referred to as late dark rearing [LDR]), leads to weakening of synaptic strength to 50% of LR mice and a doubling of afferent inputs onto each relay neuron (Hooks and Chen, 2006).

To assess structural changes that underlie functional plasticity during LDR, we compared RGC arbors reconstructed from LR and LDR mice (Figures 3A and 3B). Consistent with functional studies, average axon arbor length, complexity, and number of boutons/cluster and boutons/axon did not change significantly under normal LR conditions between P20 and P31 (Figures 3C–3H, black lines, and Figure S4). Analysis also revealed no significant difference in the size or complexity of axons from LR and LDR mice at P31 (Figures 3C–3E). However, there was a reduction in the degree of bouton clustering and size in deprived mice. While the average number of boutons did not differ between LR and LDR arbors (Figure 3F), the NN distance between boutons increased (Figure 3G) and the number of boutons per cluster decreased (Figure 3H). Consistent with a decrease in synaptic strength after LDR, the bouton diameter of P31 LDR axons was significantly smaller than those of LR mice (Figure 3I). Therefore, small-scale changes in the position and distribution of boutons accompany the rewiring between RGC and relay neurons in response to sensory experience, supporting the idea that bouton size and clustering correspond with the functional connectivity and strength of the retinogeniculate synapse.

Axon Refinement following Sensory-Dependent Plasticity

Finally, we extended our analysis to 1 month beyond the sensory-dependent phase of synapse remodeling (P31–P60). Remarkably, significant axon pruning occurred during this interval: total axon length, complexity, and the number of boutons/axon decreased (Figures 4A–4E), while the average diameter of the remaining boutons continued to increase (Figure 4F). In contrast to the structural refinement of the axon backbone, while NN distance decreased slightly, there was little change in bouton clustering (Figures 4G and 4H) or the number of clusters per axon (14.75 ± 5.4 versus 9.27 ± 6.0, mean ± SD for P31 and P60, respectively; $p > 0.05$ Mann-Whitney). Thus, overall structural pruning occurred only after the phase of experience-dependent synapse refinement.

To test whether the reduction in arbor complexity with age corresponded to a previously undetected change in functional connectivity, we recorded from mature mice (≥P60, Figure 4I). We found that the average single fiber strength in P60 mice was statistically indistinguishable from P31 mice (Figure 4J). However, the fiber fraction, an estimate of the number of inputs innervating a relay neuron, significantly increased largely due to a reduction in the maximal currents (P31 versus P60, in nA: Max AMPAR 4.1 ± 0.2 versus 3.02 ± 0.2; Max NMDAR 3.3 ± 0.3 versus 1.93 ± 0.2 mean ± SEM, both $p < 0.001$) (Figure 4K). The additional functional pruning at the retinogeniculate synapse between P31 and P60 is consistent with our findings of a decrease in the total number of boutons. These findings suggest that once the appropriate connections between RGCs and relay neurons have stabilized, excess axon segments and boutons are removed.

DISCUSSION

Studies of randomly labeled RGCs in cats and mice have demonstrated that after eye-specific segregation is complete, axon arbors continue to grow and elaborate in the correct LGN layer (Dhande et al., 2011; Snider et al., 1999; Sretavan and

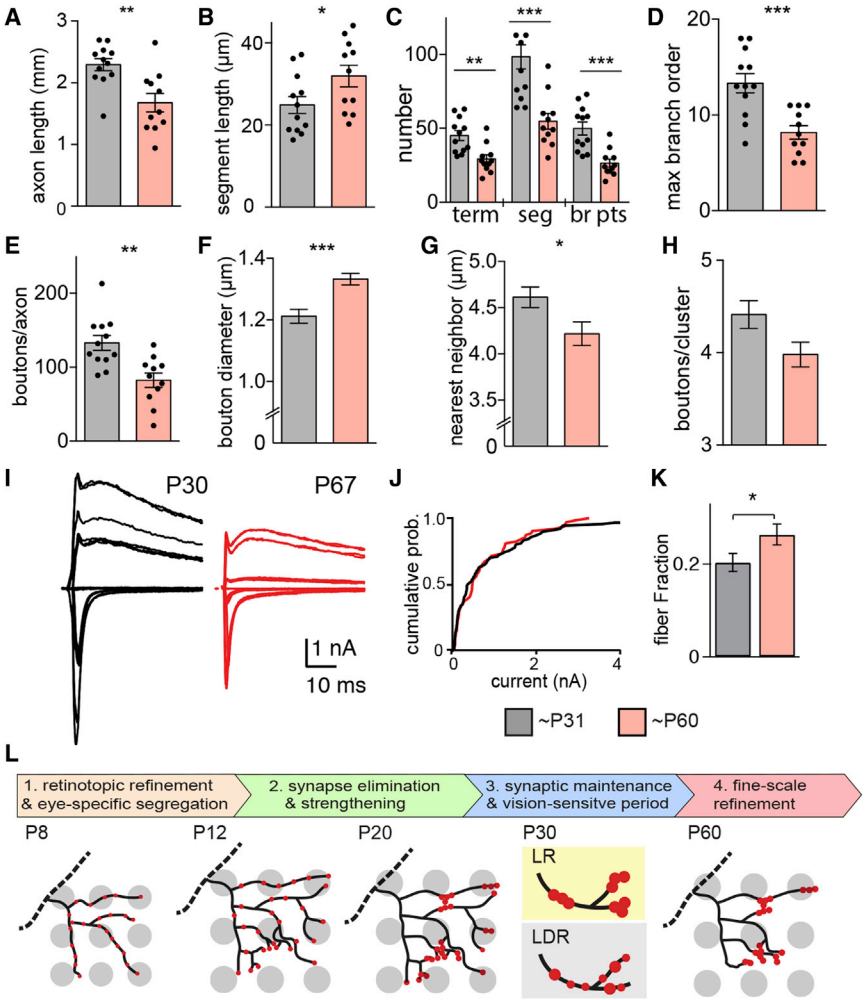

Figure 4. Structural Axonal Pruning Occurs between P31 and P60

Axon backbone (A–D) and bouton (E–H) parameters at P31 (gray) and P60 (red). P31 data set is the same as in Figure 3. (I) Representative retinogeniculate slice recordings at P30 and P67. (J) Cumulative probability distribution of single fiber AMPAR strength shows no significant difference. (K) The fiber fraction increases with age. (J and K) Gray includes P27–P34 and red P60–P75. (L) Summary schematic of structural plasticity of RGC axons in LGN. (L1) During retinotopic refinement and eye-specific segregation, the axon arbor elaborates and becomes more complex in the monocular layer. (L2) During the period of functional synapse elimination and strengthening, the overall structure of the BD-RGC axon backbone is maintained, but the synaptic boutons are redistributed to form clusters and grow in size. (L3) During the vision-sensitive period, LDR results in declustering of boutons and decrease in bouton size when compared to LR mice. (L4) Finally, between P30 and P60, further axonal and synaptic pruning takes place, with a reduction in axon size and complexity. Error bars indicate SEM. See also Figure S4.

Shatz, 1984; Sur et al., 1984). Over development, these arbors remain large despite known physiologic convergence of RGC afferents onto relay neurons (Cleland et al., 1971; Hamos et al., 1987; Mastronarde, 1992). Here we describe a previously unappreciated presynaptic mechanism of circuit refinement that explains the dissociation between structure and function. Instead of axon pruning, rewiring of a network occurs by small-scale changes in bouton position and size (summarized in Figure 4L). Rather than thinking of the immature axon structure as an imprecise attempt to make proper connections, we suggest that the axon arbor is best viewed as an opportunity map of appropriate pre- and postsynaptic connections.

Bouton Clustering

Between P8 and P20, the boutons form clusters, focusing on a small subset of the many postsynaptic neurons with which the arbor could, in principle, contact. This period corresponds to a developmental window when the number of inputs to an LGN neuron decreases by ~50% (Chen and Regehr, 2000), suggesting that clustering acts both to strengthen connections with some partners and to eliminate connections with others. By P20, when boutons have clustered, the axon backbone is larger than functionally necessary. Therefore, developmental "synapse refinement" does not simply mean the removal of synaptic contacts in the form of axon branches (Purves and Lichtman, 1980). For the postsynaptic relay cell, the total number of synaptic contacts does not change, but the presynaptic cells associated with these contacts have pruned down (Hooks and Chen, 2006).

Bouton clusters have been described in retinal axons as well as other neurons throughout the mammalian CNS (Binzegger et al., 2007; Kleindienst et al., 2011; Mason, 1982; Sur and Sherman, 1982; Takeuchi et al., 2014). Here, by fully reconstructing RGC arbors at different developmental time points, we show that bouton redistribution occurs with age. Consistent with our clustering data, reconstruction of a single RGC axon in adult cat LGN showed that a section of the arbor made synaptic contacts with only 4 of 40 possible postsynaptic partners, including >200 contacts onto one neuron (Hamos et al., 1987). Thus, bouton clustering onto the same cell, in combination with increased number of synaptic release sites within each growing bouton (Hamos et al., 1987; Yeow and Peterson, 1991), contributes to the 20-fold average strengthening of RGC inputs to LGN neurons.

RGC axon terminal morphologies in the rodent LGN vary in different LGN laminae (Erzurumlu et al., 1988); thus, it is likely that distinct forms of pruning occur among RGC subclasses (Sur et al., 1984). While we studied only one of >20 RGC subtypes in detail (BD-RGCs), we observed similar alterations in J-RGCs (Kim et al., 2008) (Figures S3I and S3J), as well as in the distribution of VGLUT2 alone, which labels synaptic boutons of most

RGC subtypes. Thus, clustering is likely to occur among non-BD RGC boutons as well. The mechanism of refinement by bouton clustering may be generalizable to other species, as bouton clusters have been well documented for RGCs in several species (Famiglietti and Peters, 1972; Ling et al., 1998). Moreover, broadening of axon arbors has been observed in randomly labeled RGCs throughout the LGN during the early stages of development (Dhande et al., 2011; Snider et al., 1999; Sretavan and Shatz, 1984).

Retinogeniculate axon reorganization is a continuous and dynamic process involving active axon branch addition and removal, in a similar manner as has been shown in other systems (Meyer and Smith, 2006; Portera-Cailliau et al., 2005; Ruthazer et al., 2006). However, our data indicate that there is no net decrease in total arbor length and complexity during the period of robust functional refinement. Rather, axon complexity increases during early stages (P8–P16) accompanied by significant clustering of presynaptic boutons. Why some synaptic connections refine by extensive die-off of terminal branches while others remodel with bouton clustering is still not clear. One possibility is that some presynaptic neurons, such as motor neurons, exclusively form synapses at the terminal end of axon branches, whereas others form en passant synapses that can undergo elimination without changing the axon backbone. With rewiring during the sensory-dependent developmental period, extension and retraction of the axon arbor could be difficult at ages when the extracellular matrix is dense and complex. Thus, a more straightforward means of remodeling a circuit may involve the addition of boutons and release sites to a preexisting large axon scaffold. In this scenario, the axon arbor structure does not accurately reflect functional connectivity.

Experience-Dependent Changes in Structure

With the onset of vision-dependent plasticity, the positions of the boutons can be adjusted along the axon arbor based on sensory experience. As in the case of LDR, small changes in bouton clustering can lead to significant rewiring of pre- and postsynaptic partners. Previous structural studies of experience-dependent plasticity in several species have focused on changes in the axon structure (Antonini and Stryker, 1993; Hua et al., 2005; Ruthazer et al., 2006). Interestingly, much like the retinogeniculate synapse, the thalamocortical axon backbone does not reflect rapid functional changes that occur in response to monocular deprivation (Antonini et al., 1999). Why functional ocular dominance plasticity precedes the shrinkage of the axon arbor by days has been a subject of ongoing debate. Studies looking for changes in synaptic density along segments of thalamocortical arbors (Silver and Stryker, 1999), or in visual cortex (Coleman et al., 2010) reported conflicting results. However, these studies did not reconstruct whole arbors to determine whether there were changes in the spatial distribution of synapses. Perhaps bouton rearrangement precedes the withdrawal of axon branches (Antonini and Stryker, 1993). Indeed, dynamic remodeling of boutons along a stable backbone has been observed in other areas accessible to time-lapse imaging (Morgan et al., 2011; De Paola et al., 2006; Stettler et al., 2006; Wierenga et al., 2008).

Late Axon Pruning

Once experience-dependent plasticity has closed, the RGC axon scaffold is reduced, limiting the potential range of pre- and postsynaptic connectivity. During this final phase of refinement, between P31 and P60, single fiber strength is unchanged, but the maximal currents decrease, leading to a more refined circuit. The number of boutons/cluster and the total number of clusters/axon do not change significantly, but the total number of boutons per axon decreases, suggesting that the elimination of boutons outside of clusters leads to the decrease in maximal current. During this phase, the removal of boutons coincides with a reduction in axon complexity. These findings are consistent with time-lapse studies in *Xenopus* showing that axon branches containing few synaptic puncta retract, while those with many puncta stabilize (Li et al., 2011; Ruthazer et al., 2006).

Conclusion

A broad axon scaffold that persists into adulthood has deep implications in development as well as in diseases involving synaptic connections. As long as the axon scaffold exists, circuit rewiring is possible. An example of the potential of an axon scaffold can be seen in barn owls whose visual field has been shifted using prisms. Young owls are able to realign their visual and auditory fields by permanently extending their axon arbor. These arbors remain broad into adulthood, and functional specificity has been proposed to arise from inhibition of inappropriate synaptic contacts and by bouton clustering (Linkenhoker et al., 2005; Zheng and Knudsen, 2001). The broad arbors allow older barn owls with previous prism experience to adapt to changes in visual maps more easily than naive birds of the same age, suggesting that the axon backbone represents a structural history of previous connections (Knudsen et al., 2000; McBride et al., 2008). Here we show that at the retinogeniculate synapse, bouton clustering underlies the development of functional specificity. However, the remnants of the RGC axon arbor may allow rapid reestablishment of previously eliminated connections during experience-dependent plasticity. With the final retraction of the axon arbor after sensory-dependent synaptic remodeling, plasticity is substantially reduced.

EXPERIMENTAL PROCEDURES

Transgenic Animals

All animal procedures were in compliance with the NIH Guide for the Care and Use of Laboratory Animals and approved by the Animal and Care and Use Program Harvard University and Children's Hospital, Boston. See details of the transgenic mouse lines used and tissue preparation and imaging protocols in Supplemental Experimental Procedures.

Bouton Distribution

Comparison of clustering was done by quantifying the nearest neighbor distance (NN) and clustering bouton positions as point processes using mean-shift clustering. See Supplemental Experimental Procedures.

Colocalization of Boutons and Synaptic Elements

Colocalization of VGLUT2 and YFP was quantified using the semiautomatic colocalization threshold and highlighter tools in ImageJ. Briefly, the colocalization highlighter used threshold values of the individual channels to create a mask for regions where YFP or VGLUT2 channels overlap. This mask was

then superimposed on the original YFP channel. The number and locations of boutons covered with the mask were counted semiautomatically using the Spots tool in Imaris as described in the "Bouton Identification" (see Supplemental Experimental Procedures).

Statistical Analysis

All data sets were evaluated for normality using the Kolmogorov-Smirnov test. For nonparametric distributions, the Mann-Whitney test was used for pairwise comparison, while the Kruskal-Wallis ANOVA with post hoc Dunn's multiple comparison test was used for groups > 2. For normally distributed data sets, we used the Student's t test and one-way ANOVA with Tukey's multiple comparison test. For all figures, $*p < 0.05$; $**p < 0.01$; $***p < 0.001$. For groups P8, P12, P16, P20, P31, P60, and LDR at P31, n = 8, 8, 8, 7, 12, 11, and 8, respectively.

SUPPLEMENTAL INFORMATION

Supplemental Information includes Supplemental Experimental Procedures and four figures and can be found with this article online at http://dx.doi.org/10.1016/j.neuron.2014.08.059.

ACKNOWLEDGMENTS

This work was supported by NIH R21EY018308, RO1 EY013613, and PO1HD18655 to C.C., RO1 NS29169 to J.S., and F31 NS055488 to Y.K.H. We thank J. Hauser, A. Thompson, J. Leffler, B.H. Lee, B.M. Hooks, J. Lichtman, T. Hensch, M. Fagiolini, and B. Stevens for helpful discussion and comments, K. Kapur for biostatistics advice, and R. Bruno for his continued patience and support for the project.

Accepted: August 29, 2014
Published: October 2, 2014

REFERENCES

Antonini, A., and Stryker, M.P. (1993). Rapid remodeling of axonal arbors in the visual cortex. Science *260*, 1819–1821.

Antonini, A., Fagiolini, M., and Stryker, M.P. (1999). Anatomical correlates of functional plasticity in mouse visual cortex. J. Neurosci. *19*, 4388–4406.

Binzegger, T., Douglas, R.J., and Martin, K.A.C. (2007). Stereotypical bouton clustering of individual neurons in cat primary visual cortex. J. Neurosci. *27*, 12242–12254.

Buffelli, M., Burgess, R.W., Feng, G., Lobe, C.G., Lichtman, J.W., and Sanes, J.R. (2003). Genetic evidence that relative synaptic efficacy biases the outcome of synaptic competition. Nature *424*, 430–434.

Chen, C., and Regehr, W.G. (2000). Developmental remodeling of the retinogeniculate synapse. Neuron *28*, 955–966.

Cheng, T.-W., Liu, X.-B., Faulkner, R.L., Stephan, A.H., Barres, B.A., Huberman, A.D., and Cheng, H.-J. (2010). Emergence of lamina-specific retinal ganglion cell connectivity by axon arbor retraction and synapse elimination. J. Neurosci. *30*, 16376–16382.

Cleland, B.G., Dubin, M.W., and Levick, W.R. (1971). Simultaneous recording of input and output of lateral geniculate neurones. Nat. New Biol. *231*, 191–192.

Coleman, J.E., Nahmani, M., Gavornik, J.P., Haslinger, R., Heynen, A.J., Erisir, A., and Bear, M.F. (2010). Rapid structural remodeling of thalamocortical synapses parallels experience-dependent functional plasticity in mouse primary visual cortex. J. Neurosci. *30*, 9670–9682.

Cruz-Martín, A., El-Danaf, R.N., Osakada, F., Sriram, B., Dhande, O.S., Nguyen, P.L., Callaway, E.M., Ghosh, A., and Huberman, A.D. (2014). A dedicated circuit links direction-selective retinal ganglion cells to the primary visual cortex. Nature *507*, 358–361.

De Paola, V., Holtmaat, A., Knott, G., Song, S., Wilbrecht, L., Caroni, P., and Svoboda, K. (2006). Cell type-specific structural plasticity of axonal branches and boutons in the adult neocortex. Neuron *49*, 861–875.

Dhande, O.S., Hua, E.W., Guh, E., Yeh, J., Bhatt, S., Zhang, Y., Ruthazer, E.S., Feller, M.B., and Crair, M.C. (2011). Development of single retinofugal axon arbors in normal and β2 knock-out mice. J. Neurosci. *31*, 3384–3399.

Erzurumlu, R.S., Jhaveri, S., and Schneider, G.E. (1988). Distribution of morphologically different retinal axon terminals in the hamster dorsal lateral geniculate nucleus. Brain Res. *461*, 175–181.

Famiglietti, E.V., Jr., and Peters, A. (1972). The synaptic glomerulus and the intrinsic neuron in the dorsal lateral geniculate nucleus of the cat. J. Comp. Neurol. *144*, 285–334.

Hamos, J.E., Van Horn, S.C., Raczkowski, D., and Sherman, S.M. (1987). Synaptic circuits involving an individual retinogeniculate axon in the cat. J. Comp. Neurol. *259*, 165–192.

Hashimoto, K., Ichikawa, R., Kitamura, K., Watanabe, M., and Kano, M. (2009). Translocation of a "winner" climbing fiber to the Purkinje cell dendrite and subsequent elimination of "losers" from the soma in developing cerebellum. Neuron *63*, 106–118.

Hong, Y.K., and Chen, C. (2011). Wiring and rewiring of the retinogeniculate synapse. Curr. Opin. Neurobiol. *21*, 228–237.

Hooks, B.M., and Chen, C. (2006). Distinct roles for spontaneous and visual activity in remodeling of the retinogeniculate synapse. Neuron *52*, 281–291.

Hooks, B.M., and Chen, C. (2008). Vision triggers an experience-dependent sensitive period at the retinogeniculate synapse. J. Neurosci. *28*, 4807–4817.

Hua, J.Y., Smear, M.C., Baier, H., and Smith, S.J. (2005). Regulation of axon growth in vivo by activity-based competition. Nature *434*, 1022–1026.

Huberman, A.D. (2007). Mechanisms of eye-specific visual circuit development. Curr. Opin. Neurobiol. *17*, 73–80.

Huberman, A.D., Manu, M., Koch, S.M., Susman, M.W., Lutz, A.B., Ullian, E.M., Baccus, S.A., and Barres, B.A. (2008). Architecture and activity-mediated refinement of axonal projections from a mosaic of genetically identified retinal ganglion cells. Neuron *59*, 425–438.

Jaubert-Miazza, L., Green, E., Lo, F.-S., Bui, K., Mills, J., and Guido, W. (2005). Structural and functional composition of the developing retinogeniculate pathway in the mouse. Vis. Neurosci. *22*, 661–676.

Kay, J.N., De La Huerta, I., Kim, I.-J., Zhang, Y., Yamagata, M., Chu, M.W., Meister, M., and Sanes, J.R. (2011). Retinal ganglion cells with distinct directional preferences differ in molecular identity, structure, and central projections. J. Neurosci. *31*, 7753–7762.

Keller-Peck, C.R., Walsh, M.K., Gan, W.B., Feng, G., Sanes, J.R., and Lichtman, J.W. (2001). Asynchronous synapse elimination in neonatal motor units: studies using GFP transgenic mice. Neuron *31*, 381–394.

Kim, I.-J., Zhang, Y., Yamagata, M., Meister, M., and Sanes, J.R. (2008). Molecular identification of a retinal cell type that responds to upward motion. Nature *452*, 478–482.

Kim, I.-J., Zhang, Y., Meister, M., and Sanes, J.R. (2010). Laminar restriction of retinal ganglion cell dendrites and axons: subtype-specific developmental patterns revealed with transgenic markers. J. Neurosci. *30*, 1452–1462.

Kleindienst, T., Winnubst, J., Roth-Alpermann, C., Bonhoeffer, T., and Lohmann, C. (2011). Activity-dependent clustering of functional synaptic inputs on developing hippocampal dendrites. Neuron *72*, 1012–1024.

Knudsen, E.I., Zheng, W., and DeBello, W.M. (2000). Traces of learning in the auditory localization pathway. Proc. Natl. Acad. Sci. USA *97*, 11815–11820.

Koch, S.M., and Ullian, E.M. (2010). Neuronal pentraxins mediate silent synapse conversion in the developing visual system. J. Neurosci. *30*, 5404–5414.

Krahe, T.E., El-Danaf, R.N., Dilger, E.K., Henderson, S.C., and Guido, W. (2011). Morphologically distinct classes of relay cells exhibit regional preferences in the dorsal lateral geniculate nucleus of the mouse. J. Neurosci. *31*, 17437–17448.

Land, P.W., Kyonka, E., and Shamalla-Hannah, L. (2004). Vesicular glutamate transporters in the lateral geniculate nucleus: expression of VGLUT2 by retinal terminals. Brain Res. *996*, 251–254.

Li, J., Erisir, A., and Cline, H. (2011). In vivo time-lapse imaging and serial section electron microscopy reveal developmental synaptic rearrangements. Neuron *69*, 273–286.

Ling, C., Schneider, G.E., and Jhaveri, S. (1998). Target-specific morphology of retinal axon arbors in the adult hamster. Vis. Neurosci. *15*, 559–579.

Linkenhoker, B.A., von der Ohe, C.G., and Knudsen, E.I. (2005). Anatomical traces of juvenile learning in the auditory system of adult barn owls. Nat. Neurosci. *8*, 93–98.

Mason, C.A. (1982). Development of terminal arbors of retino-geniculate axons in the kitten—I. Light microscopical observations. Neuroscience *7*, 541–559.

Mastronarde, D.N. (1992). Nonlagged relay cells and interneurons in the cat lateral geniculate nucleus: receptive-field properties and retinal inputs. Vis. Neurosci. *8*, 407–441.

McBride, T.J., Rodriguez-Contreras, A., Trinh, A., Bailey, R., and Debello, W.M. (2008). Learning drives differential clustering of axodendritic contacts in the barn owl auditory system. J. Neurosci. *28*, 6960–6973.

McLaughlin, T., Torborg, C.L., Feller, M.B., and O'Leary, D.D. (2003). Retinotopic map refinement requires spontaneous retinal waves during a brief critical period of development. Neuron *40*, 1147–1160.

Meyer, M.P., and Smith, S.J. (2006). Evidence from in vivo imaging that synaptogenesis guides the growth and branching of axonal arbors by two distinct mechanisms. J. Neurosci. *26*, 3604–3614.

Morgan, J.L., Soto, F., Wong, R.O.L., and Kerschensteiner, D. (2011). Development of cell type-specific connectivity patterns of converging excitatory axons in the retina. Neuron *71*, 1014–1021.

Portera-Cailliau, C., Weimer, R.M., De Paola, V., Caroni, P., and Svoboda, K. (2005). Diverse modes of axon elaboration in the developing neocortex. PLoS Biol. *3*, e272.

Purves, D., and Lichtman, J.W. (1980). Elimination of synapses in the developing nervous system. Science *210*, 153–157.

Ruthazer, E.S., Li, J., and Cline, H.T. (2006). Stabilization of axon branch dynamics by synaptic maturation. J. Neurosci. *26*, 3594–3603.

Silver, M.A., and Stryker, M.P. (1999). Synaptic density in geniculocortical afferents remains constant after monocular deprivation in the cat. J. Neurosci. *19*, 10829–10842.

Snider, C.J., Dehay, C., Berland, M., Kennedy, H., and Chalupa, L.M. (1999). Prenatal development of retinogeniculate axons in the macaque monkey during segregation of binocular inputs. J. Neurosci. *19*, 220–228.

Sretavan, D., and Shatz, C.J. (1984). Prenatal development of individual retinogeniculate axons during the period of segregation. Nature *308*, 845–848.

Stettler, D.D., Yamahachi, H., Li, W., Denk, W., and Gilbert, C.D. (2006). Axons and synaptic boutons are highly dynamic in adult visual cortex. Neuron *49*, 877–887.

Stevens, B., Allen, N.J., Vazquez, L.E., Howell, G.R., Christopherson, K.S., Nouri, N., Micheva, K.D., Mehalow, A.K., Huberman, A.D., Stafford, B., et al. (2007). The classical complement cascade mediates CNS synapse elimination. Cell *131*, 1164–1178.

Sugihara, I. (2005). Microzonal projection and climbing fiber remodeling in single olivocerebellar axons of newborn rats at postnatal days 4-7. J. Comp. Neurol. *487*, 93–106.

Sur, M., and Sherman, S.M. (1982). Retinogeniculate terminations in cats: morphological differences between X and Y cell axons. Science *218*, 389.

Sur, M., Weller, R.E., and Sherman, S.M. (1984). Development of X- and Y-cell retinogeniculate terminations in kittens. Nature *310*, 246–249.

Takeuchi, Y., Asano, H., Katayama, Y., Muragaki, Y., Imoto, K., and Miyata, M. (2014). Large-scale somatotopic refinement via functional synapse elimination in the sensory thalamus of developing mice. J. Neurosci. *34*, 1258–1270.

Tapia, J.C., Wylie, J.D., Kasthuri, N., Hayworth, K.J., Schalek, R., Berger, D.R., Guatimosim, C., Seung, H.S., and Lichtman, J.W. (2012). Pervasive synaptic branch removal in the mammalian neuromuscular system at birth. Neuron *74*, 816–829.

Wierenga, C.J., Becker, N., and Bonhoeffer, T. (2008). GABAergic synapses are formed without the involvement of dendritic protrusions. Nat. Neurosci. *11*, 1044–1052.

Winnubst, J., and Lohmann, C. (2012). Synaptic clustering during development and learning: the why, when, and how. Front Mol Neurosci *5*, 70.

Yeow, M.B., and Peterson, E.H. (1991). Active zone organization and vesicle content scale with bouton size at a vertebrate central synapse. J. Comp. Neurol. *307*, 475–486.

Zheng, W., and Knudsen, E.I. (2001). Gabaergic inhibition antagonizes adaptive adjustment of the owl's auditory space map during the initial phase of plasticity. J. Neurosci. *21*, 4356–4365.